

Wave functions and annihilation widths of heavy quarkonia

N. R. Soni,^{1,*} R. M. Parekh,¹ J. J. Patel,^{1,2,†} A. N. Gadaria,² and J. N. Pandya^{2,‡}

¹*Department of Physics, Faculty of Science, The Maharaja
Sayajirao University of Baroda, Vadodara 390002, Gujarat, INDIA.*

²*Applied Physics Department, Faculty of Technology and Engineering,
The Maharaja Sayajirao University of Baroda, Vadodara 390001, Gujarat, INDIA.*

(Dated: December 2, 2020)

Abstract

Within the framework of nonrelativistic quark-antiquark Cornell potential model formalism, we study the annihilation of heavy quarkonia. We determine their annihilation widths resulting into $\gamma\gamma$, gg , 3γ , $3g$ and γgg and compare our findings with the available theoretical results and experimental data. We also provide the charge radii and absolute square of radial Schrödinger wave function at zero quark-antiquark separation.

* nrsoni-apphy@msubaroda.ac.in

† jjpatel-apphy@msubaroda.ac.in

‡ jnpandya-apphy@msubaroda.ac.in

I. Introduction

Heavy quarkonium is the bound state of a heavy quark and a heavy antiquark that can be theoretically treated using nonrelativistic formalism. Decay properties of these states provide information regarding the internal structure as well as dynamics of the bound states. With the advancements in experimental facilities world-wide, new results for the mass spectra as well as the decay properties continue to pour in for the heavy quarkonia sector. Recently, LHCb Collaboration [1] provided the most precise measurement of ground state mass of B_c meson. Also, the excited state mass was reported by CMS Collaboration in their experimental data [2]. These results read,

$$\begin{aligned}m(B_c^+) &= 6274.47 \pm 0.27 \pm 0.17 \text{ MeV} \\m(B_c^+(2S)) &= 6871.0 \pm 1.2 \pm 0.8 \pm 0.8 \text{ MeV}\end{aligned}$$

Within the open flavor threshold, these states provide excellent opportunity for testing different theoretical approaches including effective field theories. Some of the recent approaches include attempts based on first principle such as lattice quantum chromodynamics [3–6], QCD sum rules [7, 8]. The others include perturbative QCD [9], nonrelativistic QCD [10], effective field theories [11, 12], quark models [13–15], Dyson-Schwinger and Bethe-Salpeter equation approach [16], relativistic flux tube model [17], Regge phenomenology [18, 19] as well as potential models [20–31].

In this paper, we provide the quarkonia and B_c meson wave functions at origin for ground state as well as for excited states that have been utilised for computations of various annihilation widths. This work follows our earlier work [32] in which we had made the comprehensive study of heavy quarkonia including B_c meson in the nonrelativistic potential model framework using the Cornell potential. With the help of potential parameters and numerical wave function, we have computed various decay properties such as leptonic decay constants, digamma, digluon, dilepton and electromagnetic transitions widths. This work will provide the information regarding the wave function, scalar charge radii and some weak decay properties. This study will provide the complete information regarding not only masses but also most of the annihilation widths for heavy quarkonia.

This paper is organised in the following way. After the brief information regarding the recent theoretical progress on heavy quarkonium, in Sec II, we shortly outline the nonrel-

ativistic Cornell potential model and also provide the numerical wave functions of ground state as well as the excited states. Then in Sec III, we provide the formulation for weak decays using the nonrelativistic Van Royen Weiskopf formula and in Sec. IV, we provide all the results for the annihilation widths. Finally we summarise the work presented here.

II. Formalism

For any theoretical model, it is important to predict the decay properties along with the mass spectra. Many theoretical attempts correctly predict the mass spectra but fail to reproduce the decay properties in accordance with the experiments. For computing the mass spectra of the heavy quarkonia, we choose the linear confinement along with Coulombic interaction, namely Cornell potential given by [33–35],

$$V(r) = -\frac{4}{3} \frac{\alpha_s}{r} + Ar \quad (1)$$

where α_s is the strong running coupling constant and A is the confinement strength. The Cornell potential serves as the most prominent and widely accepted potential for nonrelativistic treatment of bound states and is also supported by lattice calculations. In our earlier work [32], we had successfully employed the Cornell potential for computation of mass spectra of heavy quarkonia and B_c meson along with a range of decay properties with least number of independent model parameters, namely quark masses and confinement strengths of corresponding quarkonia states. For computation of mass spectra, we solve the Schrödinger equation numerically for Cornell potential Eq. (1) using the Runge Kutta method utilized in *Mathematica* notebook [36]. The model parameters are fixed by fitting the computed ground state masses with the corresponding experimental data. In order to compute the mass spectra of higher excited states, we add the spin dependent part of confined one gluon exchange potential perturbatively. Using the potential parameters and numerical wave function, we have computed various annihilation widths including digamma, digluon, dilepton and electromagnetic ($E1$ and $M1$) transitions. We have also computed the B_c spectroscopy using the parameters used for charmonium and bottomonium spectroscopy and our results of mass spectra are in excellent agreement with the recent data from LHCb [1]. Our results match with the ground as well as the excited state masses from LHCb [37–40] and CMS data [2]. The potential parameters used for the computation are $m_c = 1.317 \text{ GeV}$, $m_b = 4.584 \text{ GeV}$, $A_{c\bar{c}} = 0.18 \text{ GeV}^2$ and $A_{b\bar{b}} = 0.25 \text{ GeV}^2$ [32].

In this article, we provide the numerical values of the wave function of ground state as well as radial excited states at zero quark antiquark separation. This can be computed using the relation

$$R_{n\ell}^\ell(0) = \left. \frac{d^\ell R_{n\ell}(r)}{dr^\ell} \right|_{r=0}. \quad (2)$$

The wave function utilised for computation of various decay widths is mentioned above. Using the same potential parameters, we also study some additional annihilation widths such as digluon and dilepton decay width of D -wave quarkonia, 3γ , $3g$ and γgg decay widths of heavy quarkonia without using any additional parameter.

III. Determination of annihilation widths

Annihilative decays serve as the important probe for understanding the heavy quark dynamics within quarkonia. Also, they have major contribution to the total decay widths. Since these decays depend on the wave function at origin, it ultimately tests the validity of the potential. Using the potential parameters and wave function, we compute various decay properties as follows.

A. $n^3S_1 \rightarrow (3\gamma, 3g, \gamma gg)$ decay width

In the nonrelativistic limit, the annihilation widths of heavy quarkonia are directly proportional to $|R_{n\ell}^\ell(0)|^2$. The annihilation widths of S -wave vector quarkonia into gluons and photons with first order QCD radiative correction are expressed as [41–43]

$$\Gamma(n^3S_1 \rightarrow 3\gamma) = \frac{4(\pi^2 - 9)e_Q^6 \alpha^3 |R_{nsV}(0)|^2}{3\pi m_Q^2} \left(1 - \frac{12.6\alpha_s}{\pi}\right) \quad (3)$$

$$\Gamma(n^3S_1 \rightarrow \gamma gg) = \frac{8(\pi^2 - 9)e_Q^2 \alpha \alpha_s^2 |R_{nsV}(0)|^2}{9\pi m_Q^2} \left(1 - \frac{C_0 \alpha_s}{\pi}\right) \quad (4)$$

$$\Gamma(n^3S_1 \rightarrow 3g) = \frac{10(\pi^2 - 9)\alpha_s^3 |R_{nsV}(0)|^2}{81\pi m_Q^2} \left(1 - \frac{C_{0Q} \alpha_s}{\pi}\right) \quad (5)$$

where the bracketed terms are the QCD first order radiative corrections. Also $R_{nsV}(0)$ is the wave function at the origin of vector state of S -wave quarkonia. Also e_Q is the charge of heavy quark, α_s is the strong running coupling constant and α is the electromagnetic

coupling constant. The coefficients C_0 and C_{0Q} have values 6.7, 3.7 for charmonia and 7.4, 4.9 for bottomonia, respectively. The annihilation widths of S -wave vector quarkonia to 3γ , $3g$ and γgg are tabulated in Tab. II, III, IV.

B. $n^1P_1 \rightarrow 3g$ decay width

The annihilation widths P -wave to gluons state given by [42, 43] ,

$$\Gamma(n^1P_1 \rightarrow 3g) = \frac{20\alpha_s^3 |R'_{nP}(0)|^2}{9\pi m_Q^4} \ln(m_Q \langle r \rangle) \quad (6)$$

Note that for P -wave, the decay rates are proportional to the first derivative of the wave function.

C. $n^3D_1 \rightarrow e^+e^-$, $n^1D_2 \rightarrow gg$ and $n^3D_J \rightarrow 3g$ decay width

Similarly, the decay widths of D -wave heavy quarkonia to dilepton, digluon and three gluon are given by [29]. Here, the decay widths are proportional to the second derivative of the wave function.

$$\Gamma(n^3D_1 \rightarrow e^+e^-) = \frac{25e_Q^2 \alpha^2 |R''_{nD}(0)|^2}{2m_Q^4 M_{nD}^2} \left(1 - \frac{16\alpha_s}{3\pi}\right) \quad (7)$$

$$\Gamma(n^1D_2 \rightarrow gg) = \frac{2\alpha_s^2 |R''_{nD}(0)|^2}{3\pi m_Q^6} \quad (8)$$

$$\Gamma(n^3D_1 \rightarrow 3g) = \frac{760\alpha_s^3 |R''_{nP}(0)|^2}{81\pi m_Q^6} \ln(4m_Q \langle r \rangle) \quad (9)$$

$$\Gamma(n^3D_2 \rightarrow 3g) = \frac{10\alpha_s^3 |R''_{nP}(0)|^2}{9\pi m_Q^4} \ln(4m_Q \langle r \rangle) \quad (10)$$

$$\Gamma(n^3D_3 \rightarrow 3g) = \frac{40\alpha_s^3 |R''_{nP}(0)|^2}{9\pi m_Q^6} \ln(4m_Q \langle r \rangle) \quad (11)$$

The annihilation widths are listed in Tab. II - VI. Note here that in some of annihilation rates, the correction factors are not available for the higher order excited states. We compare our findings with the available PDG data as well as theoretical predictions.

IV. Results and Discussion

In this article, we have computed dilepton, digamma, digluon, 3γ , $3g$ and γgg annihilation widths of respective heavy quarkonia. For computations of these decay widths, we

have employed the respective masses and input parameters from our earlier paper [32]. For computation of mass spectra, we solve the Schrödinger equation numerically for the Cornell potential Eq. (1) and for computing the higher excited states, we perturbatively compute the spin dependent part of one gluon exchange potential. The computed masses for charmonia, bottomonia and B_c mesons are shown in Fig. 2 in comparison with experimental data. In Tab. I, we provide the absolute square of radial wave function at zero quark - antiquark separation which utilised for computations of the annihilation decay widths. The computed wave functions can also be utilised for computing the heavy quarkonium production cross sections. Using the numerical wave function, we also compute the scalar charge radii for the ground state as well as for the excited states and tabulated in Tab. I, which can be used for computations of hadronic decay widths. For computation of scalar charge radii, we use the general method given in Ref. [44, 45]. Using the potential parameters, the weak annihilation widths are computed using the leading order nonrelativistic relations including the available QCD corrections. We compare our results with available experimental data as well as different theoretical approaches. These theoretical approaches include nonrelativistic constituent quark model (NRCQM) for bottomonium spectrum [29], potential nonrelativistic quantum chromodynamics (pNRQCD) formalism in which authors have computed mass spectra and decay properties employing relativistic corrections to the Cornell potential [24]. We also compare our results with different potential model which include the Schrödinger formalism using Cornell potential for charmonia [26, 46], relativistic Dirac formalism with linear confinement [30] as well as instanton induced quarkonia potential obtained from instanton liquid model for QCD vacuum [23].

We present the non-normalised reduced wave functions of ground state as well as excited states for charmonia in Fig. 1 as examples. Similar are the plots for the bottomonia and for B_c mesons. In Tab. II, we provide the results of 3γ decay widths of charmonia and bottomonia along with different potential model and nonrelativistic constituent quark model results. For charmonia, our results are matching well with different potential model and pNRQCD potential model. Our results are also very near to the world average of experimental data from CLEO [47] and BESIII data [48]. For bottomonia, the 3γ decay width is highly suppressed and still the experimental results are not available. Our results are found to be between those reported using NRCQM and potential model results.

In Tab. III, we provide the $3g$ decay widths from various quarkonium states. For $^3S_1 \rightarrow$

$3g$, our decay widths overestimate the experimental data. For Charmonia, our results are consistent with the potential model and for bottomonia our results are matching well with potential model and NRCQM results. For P and D -wave charmonia, our results are an order higher than potential model but for bottomonia, our results are consistent with the potential models and NRCQM results.

In Tab. IV, we provide the decay widths of $n^3S_1 \rightarrow \gamma gg$ and it is observed that our results are matching fairly well with experimental data, potential model as well as NRCQM results. Similarly in Tab. V, VI, we provide the dilepton and digluon decay widths of D -wave and charmonia and bottomonia along with the results from different potential models.

V. Conclusion

In this article, we have extended our nonrelativistic treatment of heavy quarkonia for computation of annihilation of heavy quarkonia to 3γ , $3g$, γgg and e^+e^- . We utilise the model parameters and numerical wave function to compute these decay widths with QCD correction factors without using any additional parameters. Our results are very close to the experimental data and matching fairly well with the theoretical approaches such as potential models and nonrelativistic constituent quark model. We also provide the absolute square of radial wave function at zero quark-antiquark separation and scalar charge radii for ground state as well as excited states of heavy quarkonia and B_c mesons.

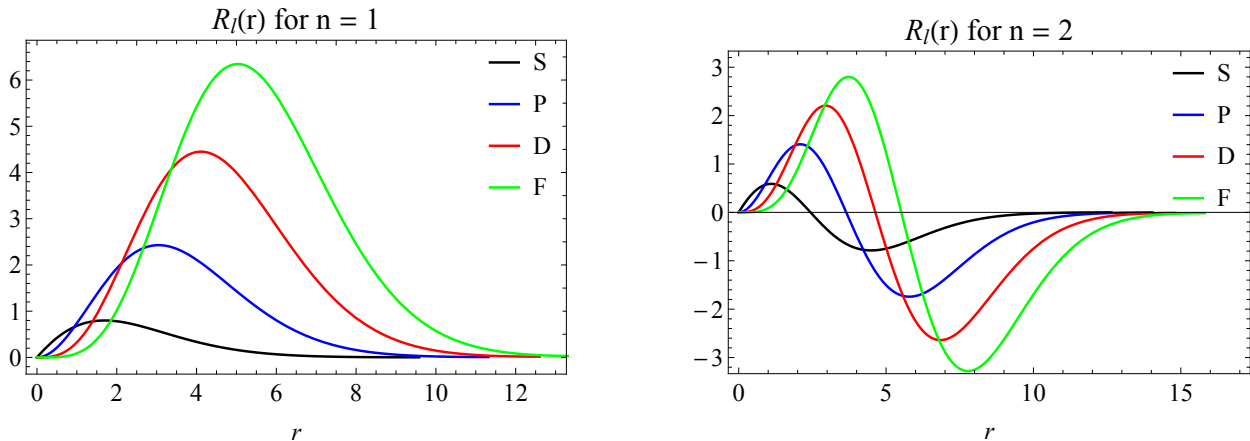


FIG. 1. Not normalised reduced wave function for charmonia

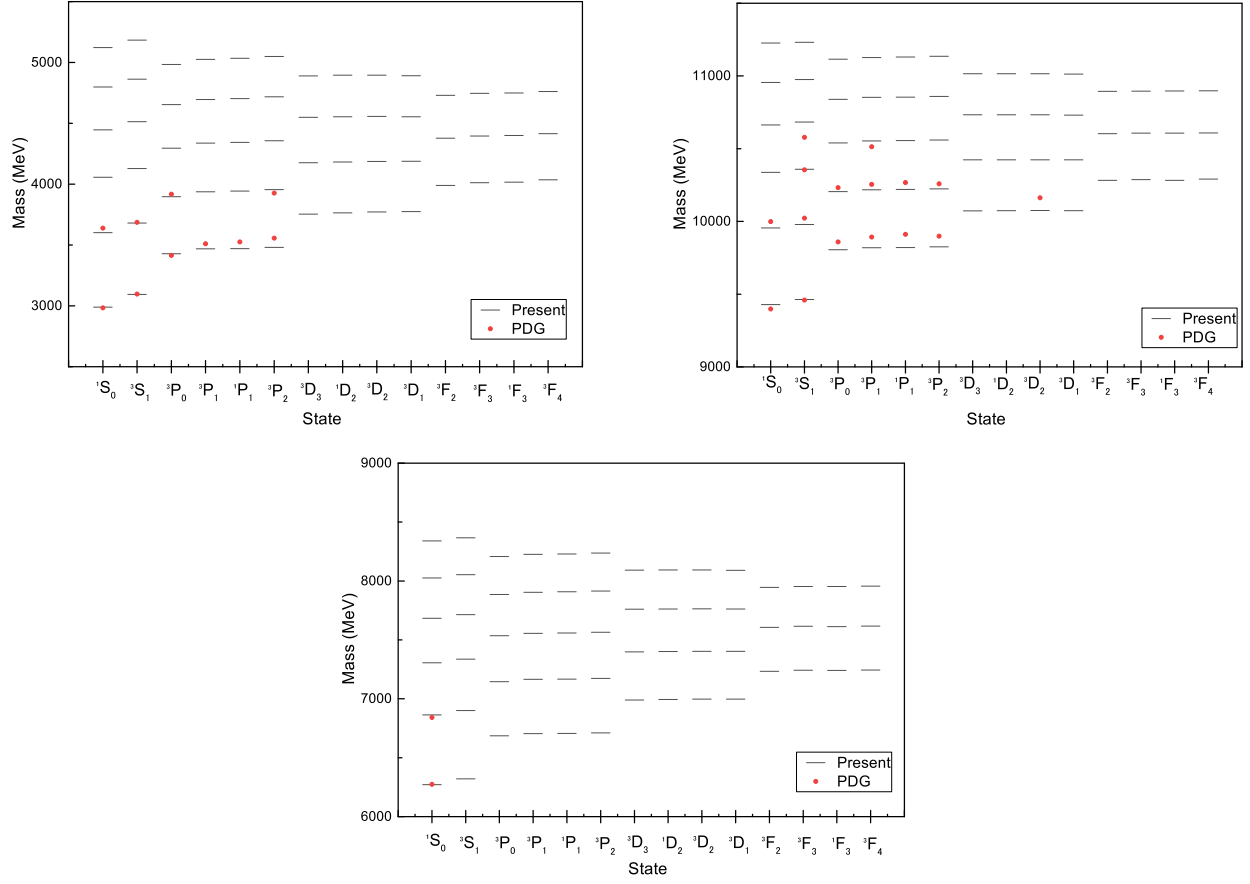


FIG. 2. Mass spectrum of charmonia (upper left), bottomonia (upper right) and B_c mesons (bottom).

Acknowledgments

J.N.P. acknowledges financial support from University Grants Commission of India under Major Research Project F.No. 42-775/2013(SR), DST-PURSE and UGC-DRS schemes.

TABLE I. Absolute square of radial wave function at origin ($|R_{nl}^{(l)}(0)|^2$ in unit of $\text{GeV}^{2\ell+3}$) and scalar charge radii ($\sqrt{\langle r^2 \rangle}$ in unit of fm) for charmonia, bottomonia and B_c mesons in unit of $\text{GeV}^{2\ell+3}$

State	$c\bar{c}$		$c\bar{b}$		$b\bar{b}$	
	$ R_{nl}^{(l)}(0) ^2$	$\sqrt{\langle r^2 \rangle}$	$ R_{nl}^{(l)}(0) ^2$	$\sqrt{\langle r^2 \rangle}$	$ R_{nl}^{(l)}(0) ^2$	$\sqrt{\langle r^2 \rangle}$
1S	0.6396	0.463	1.2457	0.373	4.1438	0.259
2S	0.4775	0.887	0.9156	0.719	2.8162	0.512
3S	0.4282	1.231	0.8167	0.999	2.4496	0.716
4S	0.4024	1.532	0.7653	1.245	2.2641	0.895
5S	0.3859	1.806	0.7325	1.468	2.1474	1.058
6S	0.3741	2.061	0.7091	1.676	2.0652	1.209
1P	0.0934	0.706	0.1753	0.572	0.4867	0.407
2P	0.0948	1.080	0.1773	0.877	0.4859	0.629
3P	0.0947	1.398	0.1770	1.136	0.4817	0.818
4P	0.0958	1.682	0.1763	1.368	0.4778	0.986
5P	0.0944	1.945	0.1757	1.581	0.4747	1.141
1D	0.0291	0.902	0.8626	0.733	0.4382	0.525
2D	0.0486	1.246	0.1376	1.013	0.7248	0.729
3D	0.0646	1.546	0.1827	1.257	0.9577	0.907
4D	0.0786	1.819	0.2222	1.479	1.1610	1.068
1F	1.1571×10^{-5}	1.077	7.5916×10^{-5}	0.875	0.0016	0.630
2F	3.4380×10^{-5}	1.399	2.2501×10^{-4}	1.137	0.0046	0.820
3F	6.7986×10^{-5}	1.685	4.4413×10^{-4}	1.370	0.0090	0.989
4F	11.2058×10^{-5}	1.949	7.3102×10^{-4}	1.585	0.0147	1.145

TABLE II. 3γ decay widths of charmonia (in eV) and bottomonia (in 10^{-6} keV)

		pNRQCD				PM	PM	PDG			
State	Present	[24]	[46]	[26]	[49]			State	Present	[23]	[29]
J/ψ	1.36	1.02	3.95	2.997	1.08 ± 0.032			$\Upsilon(1S)$	7.05	123.12	3.44
$\psi(2S)$	1.01	0.90	1.64	1.083	–			$\Upsilon(2S)$	4.79	89.89	2.00
$\psi(3S)$	0.91	0.86	1.39	1.046	–			$\Upsilon(3S)$	4.16	72.04	1.55
$\psi(4S)$	0.85	0.83	1.30	0.487	–			$\Upsilon(4S)$	3.85	60.34	1.29
$\psi(5S)$	0.81	0.81	1.25	0.381	–			$\Upsilon(5S)$	3.64	52.02	–
$\psi(6S)$	0.79	0.80	1.22	0.312	–			$\Upsilon(6S)$	3.51	44.93	–

TABLE III. $3g$ decay widths of charmonia (in keV) and bottomonia (in keV)

State	PM PDG			State	PM NRCQM PDG			
	Present	[46]	[49]		Present	[23]	[29]	[49]
J/ψ	264.25	269.06	59.55	$\Upsilon(1S)$	39.15	40.0	41.63	–
$\psi(2S)$	196.05	112.03	31.16	$\Upsilon(2S)$	26.59	26.9	24.25	18.80
$\psi(3S)$	175.43	94.57	–	$\Upsilon(3S)$	23.13	20.6	18.76	7.25
$\psi(4S)$	164.66	88.44	–	$\Upsilon(4S)$	21.37	16.8	15.58	–
$\psi(5S)$	157.77	85.30	–	$\Upsilon(5S)$	20.27	14.1	–	–
$\psi(6S)$	152.86	83.19	–	$\Upsilon(6S)$	19.49	11.7	–	–
$h_c(1P)$	1129.11	285.127		$h_b(1P)$	14.91	35.7	35.26	
$h_c(2P)$	1459.74	420.078		$h_b(2P)$	17.76	34.6	52.70	
$h_c(3P)$	1649.05	558.780		$h_b(3P)$	19.33	33.1	62.14	
$h_c(4P)$	2098.68	–		$h_b(4P)$	20.40	32.7	–	
$\psi(1D)$	1758.46	189.367		$\Upsilon(1D)$	4.667	10.6	9.97	
$\psi_2(1D)$	208.239	53.876		$\Upsilon_2(1D)$	0.552	–	0.62	
$\psi_3(1D)$	832.956	89.700		$\Upsilon_3(1D)$	2.211	6.0	0.22	
$\psi(2D)$	3231.11	359.346		$\Upsilon(2D)$	8.370	11.9	9.69	
$\psi_2(2D)$	382.632	102.236		$\Upsilon_2(2D)$	0.991	–	0.61	
$\psi_3(2D)$	1530.53	170.217		$\Upsilon_3(2D)$	3.965	5.6	1.25	
$\psi(3D)$	4588.97	556.588		$\Upsilon(3D)$	11.630	11.8	–	
$\psi_2(3D)$	539.878	158.353		$\Upsilon_2(3D)$	1.377	–	–	
$\psi_3(3D)$	2159.51	263.647		$\Upsilon_3(3D)$	5.509	5.1	–	

TABLE IV. γgg decay widths of charmonia (in keV) and bottomonia (in keV)

PM PDG				PM NRCQM PDG				
State	Present	[46]	[49]	State	Present	[23]	[29]	[49]
J/ψ	9.72	8.90	8.17	$\Upsilon(1S)$	0.85	0.72	0.79	1.18
$\psi(2S)$	7.21	3.75	3.03	$\Upsilon(2S)$	0.58	0.49	0.46	0.60
$\psi(3S)$	6.46	3.16	–	$\Upsilon(3S)$	0.50	0.39	0.36	0.01
$\psi(4S)$	6.06	2.96	–	$\Upsilon(4S)$	0.46	0.32	0.30	–
$\psi(5S)$	5.81	2.85	–	$\Upsilon(5S)$	0.44	0.27	0.25	–
$\psi(6S)$	5.63	2.78	–	$\Upsilon(6S)$	0.42	0.23	0.22	–

 TABLE V. dilepton decay widths of charmonia (in keV) and bottomonia (in 10^{-3} keV)

State	Present	PM [30]	PM [46]	State	Present	PM [30]	PM [23]	NRCQM [29]
$\psi(1D)$	0.091	0.27	0.113	$\Upsilon(1D)$	0.72	106	5.0	1.40
$\psi(2D)$	0.124	0.17	0.166	$\Upsilon(1D)$	1.12	78	5.8	2.50
$\psi(3D)$	0.139	0.099	0.211	$\Upsilon(1D)$	1.39	51	5.9	–
$\psi(4D)$	0.147	0.064	–	$\Upsilon(1D)$	1.60	42	5.8	–

 TABLE VI. digluon decay widths of D -wave charmonia (in keV) and bottomonia (in keV)

State	Present	PM [46]	State	Present	NRCQM [29]
$\eta_{c2}(1D)$	122.194	12.460	$\eta_{b2}(1D)$	0.42	0.37
$\eta_{c2}(2D)$	203.845	21.679	$\eta_{b2}(1D)$	0.69	0.67
$\eta_{c2}(3D)$	270.943	31.757	$\eta_{b2}(1D)$	0.91	–
$\eta_{c2}(4D)$	329.790	–	$\eta_{b2}(1D)$	1.11	–

-
- [1] R. Aaij *et al.* (LHCb Collaboration), JHEP **07**, 123 (2020), arXiv:2004.08163 [hep-ex].
- [2] A. M. Sirunyan *et al.* (CMS Collaboration), Phys. Rev. Lett. **122**, 132001 (2019), arXiv:1902.00571 [hep-ex].
- [3] Y. Meng, C. Liu, and K.-L. Zhang, Phys. Rev. D **102**, 054506 (2020), arXiv:1910.11597 [hep-lat].
- [4] C. Liu, Y. Meng, and K.-L. Zhang, Phys. Rev. D **102**, 034502 (2020), arXiv:2004.03907 [hep-lat].
- [5] R. Lewis and R. Woloshyn, Phys. Rev. D **85**, 114509 (2012), arXiv:1204.4675 [hep-lat].
- [6] M. Wurtz, R. Lewis, and R. Woloshyn, Phys. Rev. D **92**, 054504 (2015), arXiv:1505.04410 [hep-lat].
- [7] T. Aliev, T. Barakat, and S. Bilmis, Nucl. Phys. B **947**, 114726 (2019), arXiv:1905.11750 [hep-ph].
- [8] K. Azizi and J. Söngü, J. Phys. G **46**, 035001 (2019), arXiv:1711.04288 [hep-ph].
- [9] Y. Kiyo and Y. Sumino, Phys. Lett. B **730**, 76 (2014), arXiv:1309.6571 [hep-ph].
- [10] V. Mateu, P. G. Ortega, D. R. Entem, and F. Fernández, Eur. Phys. J. C **79**, 323 (2019), arXiv:1811.01982 [hep-ph].
- [11] N. Brambilla, W. K. Lai, J. Segovia, and J. Tarrús Castellà, Phys. Rev. D **101**, 054040 (2020), arXiv:1908.11699 [hep-ph].
- [12] N. Brambilla, H. S. Chung, D. Müller, and A. Vairo, JHEP **04**, 095 (2020), arXiv:2002.07462 [hep-ph].
- [13] P. G. Ortega, J. Segovia, D. R. Entem, and F. Fernandez, Eur. Phys. J. C **80**, 223 (2020), arXiv:2001.08093 [hep-ph].
- [14] Q. Li, M.-S. Liu, L.-S. Lu, Q.-F. Lü, L.-C. Gui, and X.-H. Zhong, Phys. Rev. D **99**, 096020 (2019), arXiv:1903.11927 [hep-ph].
- [15] D. Ebert, R. Faustov, and V. Galkin, Eur. Phys. J. C **71**, 1825 (2011), arXiv:1111.0454 [hep-ph].
- [16] M. Chen, L. Chang, and Y.-x. Liu, Phys. Rev. D **101**, 056002 (2020), arXiv:2001.00161 [hep-ph].
- [17] B. Chen, A. Zhang, and J. He, Phys. Rev. D **101**, 014020 (2020), arXiv:1910.06065 [hep-ph].

- [18] A. Badalian and B. Bakker, Phys. Rev. D **100**, 054036 (2019), arXiv:1902.09174 [hep-ph].
- [19] J.-K. Chen, Eur. Phys. J. C **78**, 235 (2018).
- [20] D. Molina, M. De Sanctis, C. Fernández-Ramírez, and E. Santopinto, Eur. Phys. J. C **80**, 526 (2020), arXiv:2001.05408 [hep-ph].
- [21] E. J. Eichten and C. Quigg, (2019), arXiv:1904.11542 [hep-ph].
- [22] E. J. Eichten and C. Quigg, Phys. Rev. D **99**, 054025 (2019), arXiv:1902.09735 [hep-ph].
- [23] B. Pandya, M. Shah, and P. C. Vinodkumar, (2019), arXiv:1910.06111 [hep-ph].
- [24] R. Chaturvedi and A. K. Rai, Int. J. Theor. Phys. **59**, 3508 (2020), arXiv:1910.06025 [hep-ph].
- [25] R. Chaturvedi, A. K. Rai, N. R. Soni, and J. N. Pandya, J. Phys. G **47**, 115003 (2020).
- [26] R. Chaturvedi and A. Kumar Rai, Eur. Phys. J. Plus **133**, 220 (2018).
- [27] W.-J. Deng, H. Liu, L.-C. Gui, and X.-H. Zhong, Phys. Rev. D **95**, 074002 (2017), arXiv:1607.04696 [hep-ph].
- [28] W.-J. Deng, H. Liu, L.-C. Gui, and X.-H. Zhong, Phys. Rev. D **95**, 034026 (2017), arXiv:1608.00287 [hep-ph].
- [29] J. Segovia, P. G. Ortega, D. R. Entem, and F. Fernández, Phys. Rev. **D93**, 074027 (2016), arXiv:1601.05093 [hep-ph].
- [30] T. Bhavsar, M. Shah, and P. C. Vinodkumar, Eur. Phys. J. **C78**, 227 (2018), arXiv:1803.07249 [hep-ph].
- [31] J. N. Pandya, N. R. Soni, N. Devlani, and A. K. Rai, Chin. Phys. C **39**, 123101 (2015), arXiv:1412.7249 [hep-ph].
- [32] N. Soni, B. Joshi, R. Shah, H. Chauhan, and J. Pandya, Eur. Phys. J. C **78**, 592 (2018), arXiv:1707.07144 [hep-ph].
- [33] E. Eichten, K. Gottfried, T. Kinoshita, J. B. Kogut, K. Lane, and T.-M. Yan, Phys. Rev. Lett. **34**, 369 (1975), [Erratum: Phys.Rev.Lett. 36, 1276 (1976)].
- [34] E. Eichten, K. Gottfried, T. Kinoshita, K. Lane, and T.-M. Yan, Phys. Rev. Lett. **36**, 500 (1976).
- [35] E. Eichten, K. Gottfried, T. Kinoshita, K. Lane, and T.-M. Yan, Phys. Rev. D **17**, 3090 (1978), [Erratum: Phys.Rev.D 21, 313 (1980)].
- [36] W. Lucha and F. F. Schoberl, Int. J. Mod. Phys. **C10**, 607 (1999), arXiv:hep-ph/9811453 [hep-ph].

- [37] R. Aaij *et al.* (LHCb Collaboration), Phys. Rev. Lett. **122**, 232001 (2019), arXiv:1904.00081 [hep-ex].
- [38] R. Aaij *et al.* (LHCb Collaboration), Phys. Rev. D **95**, 032005 (2017), arXiv:1612.07421 [hep-ex].
- [39] R. Aaij *et al.* (LHCb Collaboration), Phys. Rev. Lett. **113**, 152003 (2014), arXiv:1408.0971 [hep-ex].
- [40] R. Aaij *et al.* (LHCb Collaboration), Phys. Rev. D **87**, 112012 (2013), [Addendum: Phys.Rev.D 89, 019901 (2014)], arXiv:1304.4530 [hep-ex].
- [41] R. Van Royen and V. F. Weisskopf, Nuovo Cim. A **50**, 617 (1967), [Erratum: Nuovo Cim.A51,583(1967)].
- [42] W. Kwong, P. B. Mackenzie, R. Rosenfeld, and J. L. Rosner, Phys. Rev. D **37**, 3210 (1988).
- [43] W. Kwong and J. L. Rosner, Phys. Rev. D **38**, 279 (1988).
- [44] P. C. Vinodkumar, J. N. Pandya, V. M. Bannur, and S. B. Khadkikar, Eur. Phys. J. A **4**, 83 (1999).
- [45] J. N. Pandya and P. C. Vinodkumar, Pramana **57**, 821 (2001).
- [46] V. Kher and A. K. Rai, Chin. Phys. C **42**, 083101 (2018), arXiv:1805.02534 [hep-ph].
- [47] D. Besson *et al.* (CLEO Collaboration), Phys. Rev. D **78**, 032012 (2008), arXiv:0806.0315 [hep-ex].
- [48] M. Ablikim *et al.* (BESIII Collaboration), Phys. Rev. D **87**, 032003 (2013), arXiv:1208.1461 [hep-ex].
- [49] M. Tanabashi *et al.* (Particle Data Group), Phys. Rev. D **98**, 030001 (2018).